Cell-Surface Aminopeptidases: Basic and Clinical Aspects.
S. Mizutani et al., editors.

DPPIV/CD26: structural and biological characteristics of asparagine and cysteine mutants*

Hua Fan, Joerg Dobers and Werner Reutter
Institut für Molekularbiologie und Biochemie, Freie Universität Berlin, Berlin-Dahlem, Germany

Abstract. *Background.* Dipeptidyl peptidase IV (DPPIV/CD26) is a highly glycosylated type II membrane protein. In addition to its highly specific ectopeptidase activity it also functions in cell adhesion, differentiation and T-cell activation. The extracellular domain of rat DPPIV contains eight N-glycosylation sites and twelve cysteine residues, and it can be divided into three distinctive regions.

Methods. Each N-glycosylation site and cysteine residue was eliminated by site-directed mutagenesis. Mutants were expressed and characterized with respect to cellular localisation, N-glycan processing, stability, enzymatic activity and dimer formation. The number of free thiol groups in the native enzyme was determined chemically.

Results. We found that N-glycosylation is important for the stability and processing of the molecule. The glycans are involved in DPPIV-mediated adhesion to collagen type I. Mutations of the N-glycosylation site, at 319, and of cysteines 326, 337, 448, 455 and 552 altered the biochemical properties of DPPIV dramatically. Chemical titration revealed the existence of six free thiol groups in native DPPIV; the respective six cysteine residues may associate to form disulfide bridges.

Conclusion. Our results suggest that the cotranslational N-glycosylation at position 319 and the presence of cysteine residues 326, 337, 445, 448, 455 and 552 are necessary for the correct folding and functional conformation of this molecule.

Keywords: dipeptidyl peptidase IV, disulfide bridge, N-glycosylation, structure-function relationship.

Introduction

The multifunctional type II transmembrane glycoprotein, dipeptidyl peptidase IV (DPPIV, E.C.3.4.14.5), is expressed by nearly all mammalian cells. First described as glycyl-prolyl-naphthylamidase, by Hopsu-Havu and Glenner, from rat liver [1,2], it has been shown to be an activation marker on lymphocytes and other immune cells [3—5]. The sequences of DPPIV-isoforms from human and mouse exhibit very high similarities [6,7]. Soluble forms exist, e.g., in lysosomes, in human serum [8,9] and in *Xenopus laevis* [10].

The membrane-bound wild-type rat enzyme is expressed as a noncovalently linked 210-kDa homodimer at the cell surface [11]. Whether dimerization occurs prior to Golgi import [12] or in the late Golgi-apparatus [13] is still not known.

Address for correspondence: Dr Werner Reutter, Institut für Molekularbiologie und Biochemie, Freie Universität Berlin, Arnimallee 22, 14195 Berlin-Dahlem, Germany. Tel.: +49-30-8445-1565. Fax: +49-30-8445-1541. E-mail: reutter@medizin.fu-berlin.de
*Note: a web page is available at http://www.fu-berlin.de/sfb366/

Rat-DPPIV consists of a short cytoplasmic domain, followed by a hydrophobic transmembrane domain and an extracellular sequence of 739 amino acids [14]. The primary structure contains eight potential N-glycosylation sites, five of them proximal to the transmembrane domain. The glycan-rich domain is followed by a cysteine-rich region containing ten of the twelve cysteine residues. The active site with the catalytic triad is located near the carboxy-terminus (Fig. 1) [15,16].

Besides its well-known exopeptidase activity, DPPIV also exhibits endopeptidase activity towards denatured collagen [17]. Its very distinct substrate specificity is important for the processing and modulation of defined peptides and chemokines [18]. Expression of DPPIV/CD26 is closely associated with cell adhesion [19,20] and differentiation [21]. It displays important costimulatory properties during T-cell activation and proliferation. The specific interaction of CD26 with extracellular adenosine deaminase (ADA) has been shown to significantly modulate immune activity in humans [3,22].

The biological significance of N-glycosylation and the resulting N-glycans of DPPIV is not fully understood. The cysteine-rich domain of DPPIV mediates binding to ADA and collagen [23]. The tertiary structure of DPPIV is unknown, but initial studies on its elucidation have been reported [24–26]. In the present work, we investigated the influence of N-glycosylation and cysteine residues on the structural and biological properties of the protein.

Materials and Methods

Purification of DPPIV from plasma membranes and titration of free sulfhydryl groups

Native DPPIV from the livers of adult male Wistar rats was purified by concavalin A– and immunoaffinity chromatography as described earlier [27]. Purified DPPIV was titrated with 5,5'-dithiobis-(2-nitrobenzoic acid) (DTNB) according to Pecci et al. [28]. Titrations were performed under native (0.1 M Tris/HCl, pH 7.8) or denaturing (6.4 M guanidinium/HCl, pH 6.0) conditions at 25°C for up to 4 h.

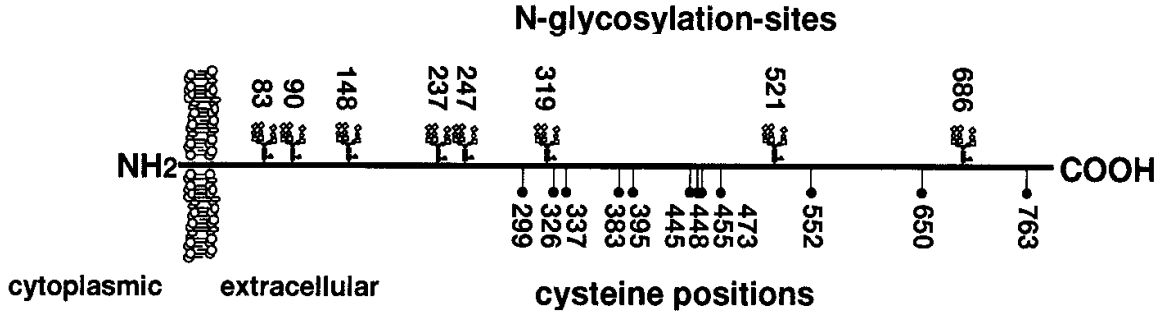

Fig. 1. Schematic primary structure of rat DPPIV with N-glycosylation-sites and cysteine positions.

Construction of mutant DPPIV

Each point-mutation was generated by site-directed mutagenesis with synthetic oligonucleotides bearing the desired mutation. Mutations N89Q, N319Q, N686Q and C326G were generated with the Amersham Sculptor-system [29]. The cysteine mutations were performed using the Stratagene Quikchange-system [30].

Transfection, flow cytometry and the sorting of stable CHO transfectants

Transfections were performed using the Eppendorf Multiporator and an appropriate Eppendorf protocol. Transfectants were selected with geneticin G418. For immunostaining, polyclonal antiserum against wild-type DPPIV or monoclonal antibody 13.4 (mAb 13.4) against the cysteine-rich domain of DPPIV was used. Cells were incubated with fluorescein isothiocyanate (FITC)-labeled rabbit antimouse (for mAb 13.4) and goat antirabbit IgG (for polyclonal antibodies), then analysed using a FACScan flow cytometer (Becton Dickinson). Surviving positive cells were selected with the FACS Vantage cell-sorter.

^{35}S-labelling of DPPIV by the pulse-chase method

Pulse-chase experiments were performed as described earlier [29]. In the case of Endo H treatment, cells were pulse-labeled for 30 min, then chased for various periods. Polyclonal anti-DPPIV IgG or mAb 13.4 was used for immunoprecipitation. The radioactivity of protein bands was quantified on a Phosphor Imager (Molecular Dynamics) with the aid of IPLabGel-Software.

Endoglycosidase H (Endo H) treatment

After the ^{35}S-labeling and immunoprecipitation of DPPIV with mAb 13.4, precipitates were eluted by boiling for 4 min in buffer containing 0.4% SDS, 1% β-mercapto-propanediol and 40 mM EDTA. One-half of the eluted protein was treated with Endo H (0.02 unit/80 ml) at 37°C for 16 h in 50 mM acetate buffer, pH 5.5.

Immunofluorescence microscopy

Cells were fixed with 3% v/v formaldehyde in NaCl/Pi at room temperature (RT) for 10 min (if indicated, after permeabilization with 0.1% Triton X-100 in NaCl/Pi at RT for 5 min), then blocked with 0.1 M glycine in NaCl/Pi for 30 min. Anti-DPPIV polyclonal antibodies and mAb 13.4 were used for immunostaining. After washing, the cells were incubated with FITC-conjugated rabbit antimouse IgG antibodies.

Other methods

For Western blot analysis, immunostaining was performed with mAb 13.4 or polyclonal antibodies and visualized by chemiluminescence. For immunoprecipitation, the supernatant was incubated with protein A-Sepharose-bound mAb 13.4, or protein A-Sepharose-bound polyclonal antibodies for 12 h at 4°C. Enzymatic activity was determined as described, with Gly-Pro-4-nitroanilide as the substrate [31]. Protein crosslinking was performed with the homobifunctional disuccinimidylsuberate as described earlier [30]. To normalize differences in the expression level, DPPIV Western blots were performed in parallel and the intensities of bands at 100 and 110 kDa were determined with IPLabGel software.

Results

N-Glycosylation is important for biological stability of DPPIV

In order to study the influence of N-glycosylation on the protein stability, the half-lives ($t_{1/2}$) of N-glycosylation mutants of DPPIV were analysed by pulse-chase experiments. As shown in Fig. 2, wild-type DPPIV is very stable with a $t_{1/2}$ of 55 h, as previously reported by Hong et al. [32]. In contrast, the N-glycosylation mutants of DPPIV are less stable; most $t_{1/2}$ are in the range of 20 to 40 h, but the $t_{1/2}$ of N319Q is much shorter, being only about 10% of the value for wild-type DPPIV.

Defective N-glycosylation delays processing and translocation of DPPIV

In order to confirm the above interpretation, we performed pulse-chase experiments with transfected wild-type DPPIV and DPPIV N-glycosylation mutants and digested the immunoprecipitated peptides with Endo H. Glycoproteins containing only mannose-rich glycans are Endo H-sensitive, whereas hybrid or mature complex forms are Endo H-resistant.

Figure 3 shows that after a 30 min pulse, 50% of the oligosaccharides of wild-type DPPIV had been processed to a mature complex form, whereas the corresponding values for N83Q and N686Q were 25 to 40%, respectively. After a 60 min chase almost all of the oligosaccharides of wild-type DPPIV were processed to the mature complex form, whereas N83Q and N686Q were processed more slowly. It is interesting that most of the N319Q was converted into a polypeptide of apparent M_r 84,000 after Endo H digestion, irrespective of the chase and sampling time; therefore, only a small proportion could be processed to a mature complex form. This result suggests that mutation at position N319 dramatically inhibits the N-glycosylation process, and the mutations at positions N83 and N686 may retard the N-glycosylation processing of this protein. Immunofluorescence microscopy shows that, as well as wild-type DPPIV, all N-glycosylation mutants, except N319Q, were expressed on the surface of transfected CHO cells

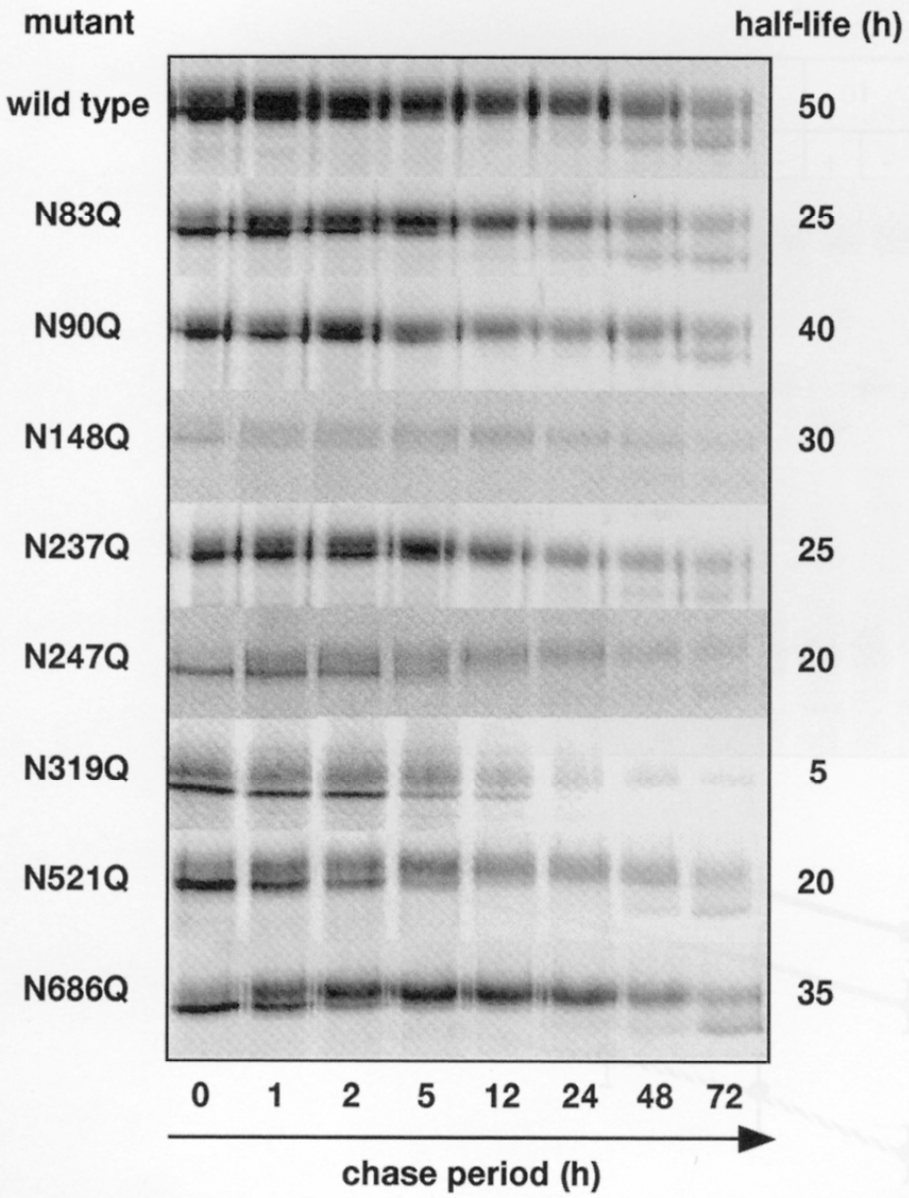

Fig. 2. Biological stability of DPPIV N-glycosylation mutants. CHO transfectants were pulse-labeled with [^{35}S]methionine for 30 min and chased for 0, 1, 2, 5, 12, 24, 48 or 72 h. Immunoprecipitates of cell lysates obtained at the indicated times of chase were analysed by SDS/PAGE. The results of the pulse-chase experiments were analysed by phosphoimager scanning.

(Fig. 4). Mutant N319Q, however, does not appear on the cell surface but is located inside the cell (Fig. 4). N319Q is concentrated near the endoplasmic reticulum (ER) suggesting that this protein cannot be translocated from the ER to the cell surface.

N-Glycans are associated with adhesion of DPPIV to collagen

CHO cells transfected with DPPIV and DPPIV N-glycosylation mutants were tested for adhesion on collagen I. Compared with nontransfected CHO cells,

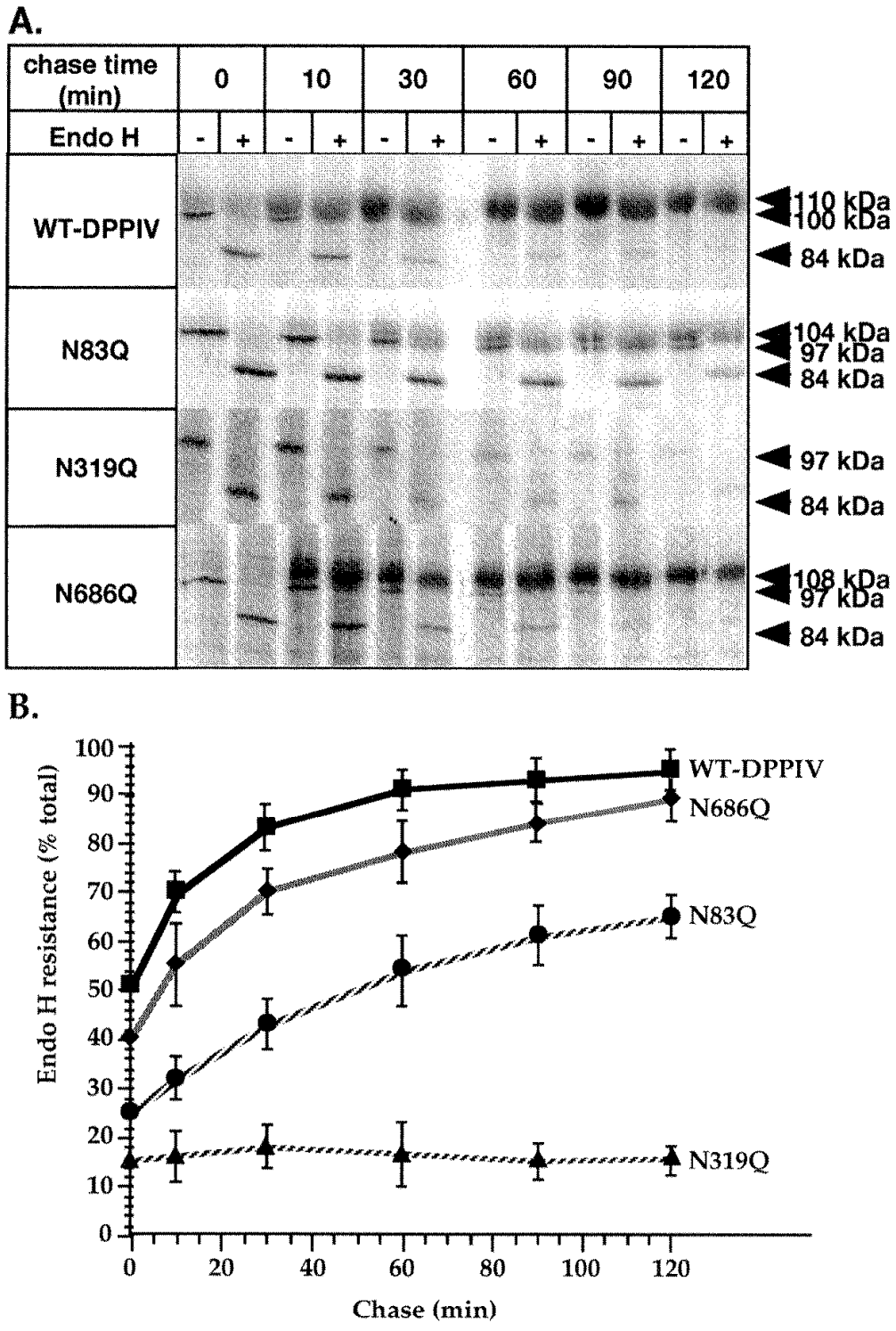

Fig. 3. Processing of DPPIV N-glycosylation mutants. **A:** CHO/wild-type DPPIV, CHO/N83Q, CHO/N319Q and CHO/N686Q were pulse-labelled with [^{35}S]methionine for 30 min and chased for 0, 10, 30, 60, 90 or 120 min. After the immunoprecipitation of DPPIV with mAb 13.4, one-half of the eluted immunoprecipitates were treated with Endo H (0.02 U/80 ml) and then analysed by SDS/PAGE. **B:** The protein bands obtained in pulse-chase experiments were quantified on a Phosphor Imager with the aid of IPLabGel-Software. The total amounts of both Endo-H-resistant and Endo-H-sensitive protein bands at each time were set as 100%.

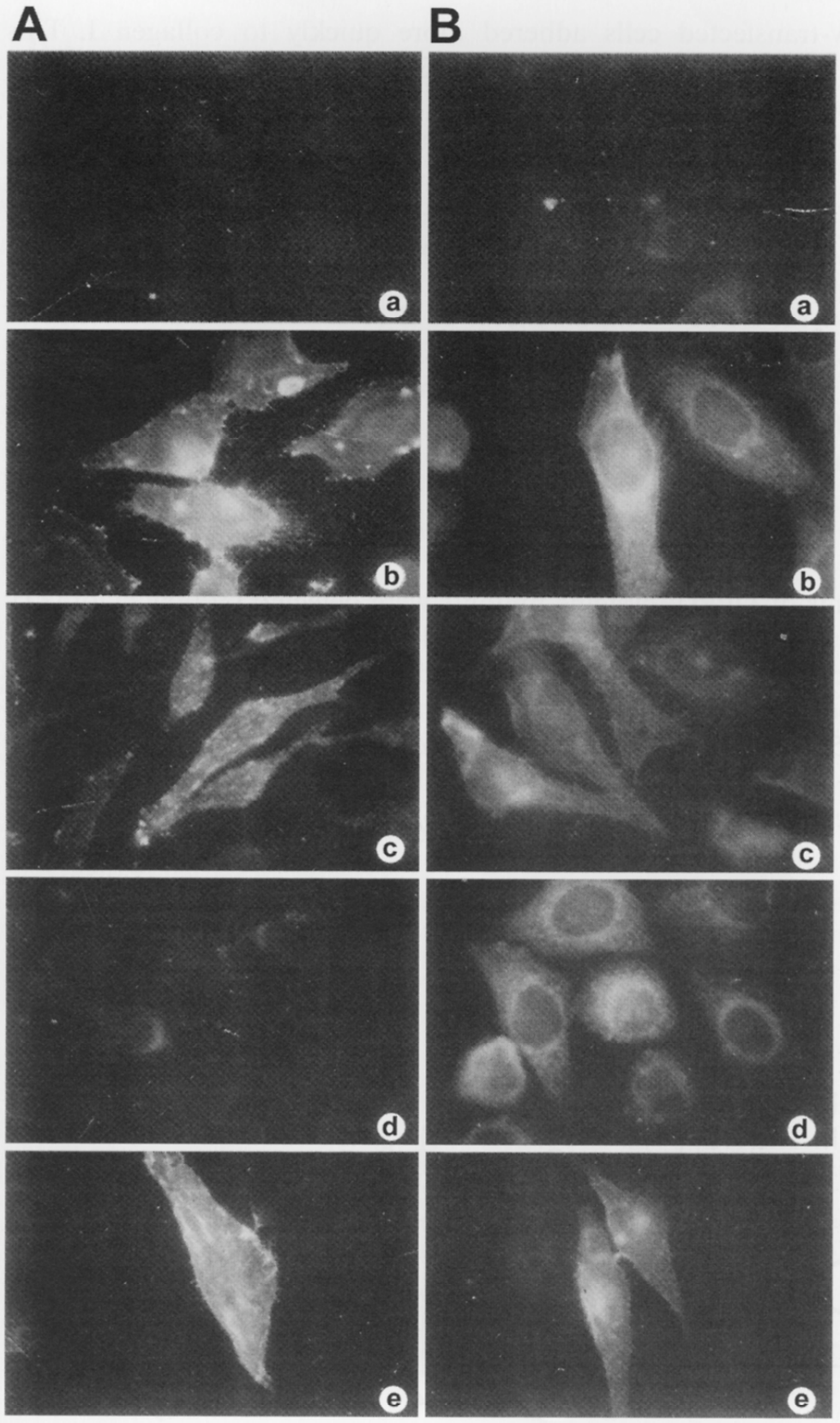

Fig. 4. Immunofluorescence microscopy of DPPIV N-glycosylation mutants. The anti-DPPIV mAb 13.4 was used for immunostaining. **A:** Cell surface staining. **B:** Cell permeability staining. CHO cells (DPPIV negative) (**a**), CHO/wild-type DPPIV (**b**), CHO/N83Q (**c**), CHO/N319Q (**d**), and CHO/N686Q (**e**).

wild-type DPPIV-transfected cells adhered more quickly to collagen I. This DPPIV-mediated effect was abolished by mAb 13.4, which is in accordance with the results of Löster et al. [27]. Compared with wild-type DPPIV transfectants, the initial adhesion of specific N-glycosylation mutants (transfectants N83Q, N148Q, N237Q) to collagen I is slower.

Native rat DPPIV contains six free cysteine residues

Titration of native rat DPPIV with an excess of DTNB showed the presence of six free sulfhydryl groups after 4 h incubation. Under denaturing conditions the titration kinetics show a higher accessibility of the SH-groups to DTNB (Fig. 5). The total of six free SH-groups could be measured either under nondenaturing or denaturing conditions.

Cysteine mutations cause conformational changes in the cysteine-rich domain

Stable transfectants of DPPIV cysteine mutants were detected by flow cytometry and selected by cell sorting. Expression of wild-type DPPIV and all cysteine mutants can be detected intracellularly and, to different extents, on the cell surface using the polyclonal anti-DPPIV antiserum. In contrast, mutants C326G, C337S and C455G were not detectable with the anti-DPPIV mAb 13.4, whose epitope is in the cysteine-rich domain of DPPIV [27]. Additionally, mAb 13.4 shows a significantly weaker affinity to C395S, C445S, C448S, C473S and

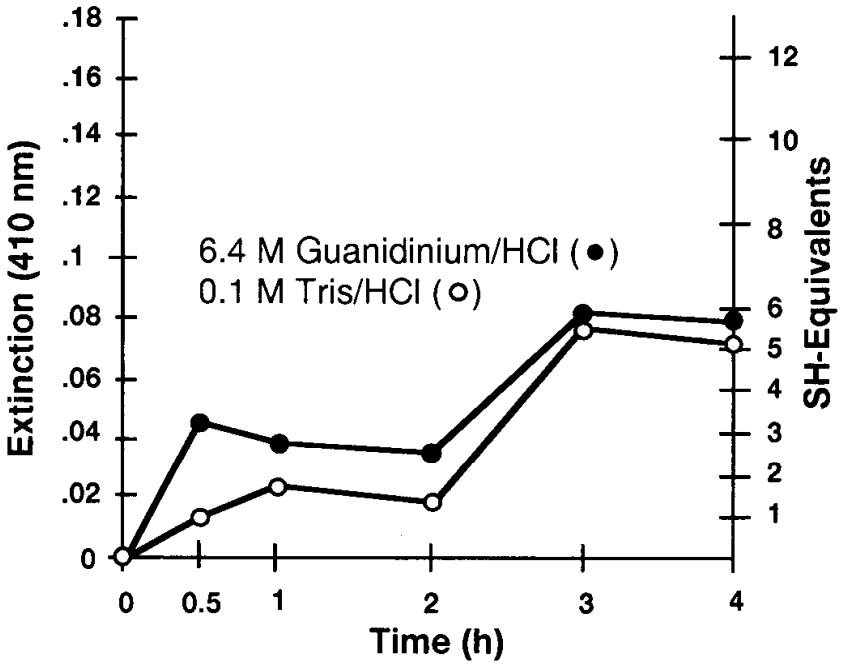

Fig. 5. Titration of native rat DPPIV reveals six free SH-groups. Experiments were performed in triplicate with 5,5'-dithiobis-(2-nitrobenzoic acid) under denaturing (6.4 M Guanidinium/HCl) and nondenaturing (0.1 M Tris/HCl) conditions.

C552S. Figure 6 exemplifies the intracellular recognition of wild-type protein and mutants C383G, C326G and C395S by FACS-analysis after mAb 13.4-staining.

Cysteine mutations influence biogenesis of DPPIV

Western blot and flow cytometry show that mutations at individual cysteine residues exert different effects on the processing and cellular localization of DPPIV. Mutants that do not develop the mature 110-kDa form are not expressed on the cell surface, so that their trafficking is different from that of wild-type DPPIV. Pulse-chase experiments revealed major differences in the $t_{1/2}$ of cysteine mutants. The $t_{1/2}$ of cysteine mutants C326G, C337S, C383S, C448S and C763S are 20 to 50% of the wild-type $t_{1/2}$ (55 h), while the $t_{1/2}$ of mutants C445S, C455G, C473S and C552S are less than 20% of the wild-type.

These quantitative changes in protein stability are reflected in significant differences in the processing and degradation kinetics of newly synthesized mutant DPPIV. Kinetics were determined by consideration of all three DPPIV-forms of 90, 100 and 110 kDa in pulse-chase experiments (Fig. 7). Wild-type DPPIV processing starts with almost equal amounts of nonprocessed 100-kDa (55%) and

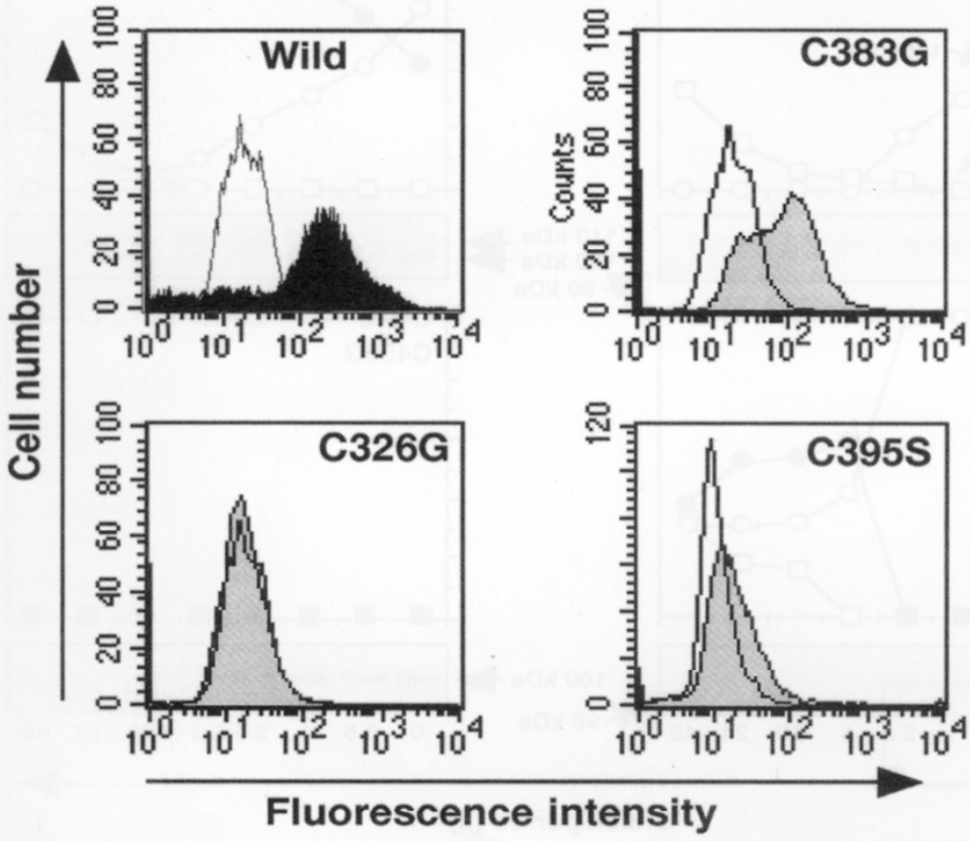

Fig. 6. The mAb 13.4 epitope is affected in distinct cysteine mutants of DPPIV. FACS-analysis of stable transfected CHO cells after intracellular staining with mAb 13.4 as first antibody. C383G: normal mAb 13.4 recognition, C326G: no recognition, C395S: reduced recognition (transfectants: hatched charts, negative-controls: clear charts).

the mature 110-kDa form (45%). The immature 100-kDa form of wild-type DPPIV is continuously processed to the mature 110-kDa form within 5 h. Mutants C299G, C383G, C395S, C650G and C763S show similar kinetics, as illustrated for C383G. Mutants C326G, C337S, C445S, C448S and C473S show a second kinetic, exemplified with C337S. The immature 100-kDa form is processed significantly more slowly and the mature 110-kDa form shows only weak stability. The processing pattern of mutant C455G is also shown in Fig. 7. This kinetic, also found at mutant C552S, is totally different because only the immature 100-kDa form is expressed over the whole chase period. Neither mature protein nor the degradation product could be detected.

Dimerization and enzymatic activity of N-glycosylation and cysteine mutants

To investigate the potential role of the mutated N-glycosylation sites and cysteine residues in the formation of the DPPIV homodimer, detergent-solubilized DPPIV

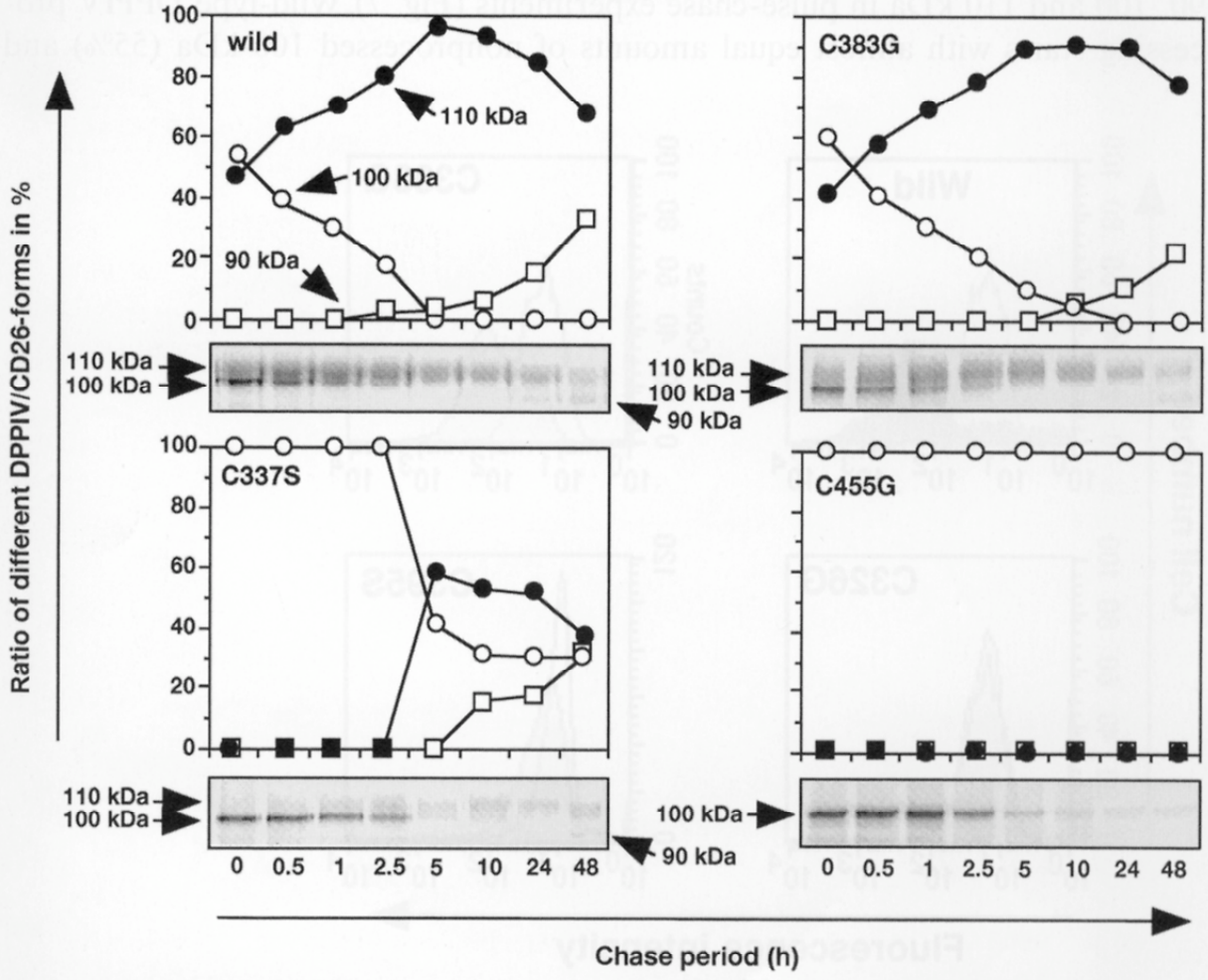

Fig. 7. Autoradiographs and protein-processing kinetics of DPPIV. Autoradiographs of pulse-chase ^{35}S-labeled and immunoprecipitated DPPIV (mutants). Protein, obtained from equal cell numbers, was subjected to reducing SDS-PAGE and Western blotting prior to autoradiography. Three different processing kinetics were computed from the autoradiographs.

mutants were incubated with the homobifunctional and noncleavable crosslinker disuccinimidylsuberate (DSS). DSS-crosslinked wild-type DPPIV consists of the 110-kDa monomeric and 210-kDa homodimeric form. All N-glycosylation mutants except N319Q and cysteine mutants C299G, C383G, C395S, C650G and C763S are also capable of dimer-formation. However, mutant N319Q is expressed as a 97-kDa protein, while cysteine mutants C326G, C337S, C445S, C448S, C455G, C473S and C552S are expressed as the 100-kDa form. Relative enzymatic activity of wild-type DPPIV was compared with the activity of N-glycosylation and cysteine-mutant proteins. Mutants which did not dimerize showed hardly any enzymatic activity.

Discussion

In this study we investigated the structural and functional significance of N-glycosylation and of cysteine residues in DPPIV/CD26. Site-directed mutagenesis was used to abolish glycosylation at single N-glycosylation sites and to modify single cysteine residues of DPPIV.

We found that defective N-glycosylation affected the biological stability and processing of the protein. The absence of only one of the N-glycosylation sites was sufficient to reduce the stability of the DPPIV protein and to retard the N-glycosylation processing to varying extents. This suggests that complete N-glycosylation is important for the protein stability and processing of DPPIV. It is possible that oligosaccharide side chains protect the protein directly against protease degradation. Another explanation would be that the mutations affect the folding and oligomerization process, resulting in a prolonged stay in the ER and an increased proteolytic breakdown in this compartment [33].

Defective glycosylation at sites Asn83, 90, 148, 237, 247, 521 and 686 had little influence on its cell-surface expression, dimerization and enzymatic activity, despite the fact that Asn686 is localized close to the active site [15,16]. In contrast, defective glycosylation of Asn319, which is located within the cysteine-rich region of DPPIV, resulted in a dramatic change of the biochemical properties and functions of this protein. This mutant, which showed hardly any enzymatic activity, could not dimerize or translocate to the cell surface; it was retained in the ER and quickly degraded after polypeptide synthesis. This molecule presumably contains only high-mannose-type N-glycans, and these are not processed into mature complex oligosaccharides. It is proposed that this mutant protein may be misfolded by the formation of aberrant intrachain disulfide bonds [34].

Chemical titration of native rat DPPIV/CD26 showed the presence of six free sulfhydryl groups. To elucidate which cysteine residues are involved in bridge formation and, therefore, relevant for DPPIV/CD26-structure we generated twelve different point mutations by site-directed mutagenesis. In each mutant, one of the twelve cysteine residues was mutated either to an inert glycine or to the structural homologue serine. Mutants C299G, C393G, C395S, C650G and C763S show wild-type-like biochemical properties, while mutations at cysteine residues

326, 337, 445, 448, 455, 473 and 552 caused a dramatic change in the biochemical properties of this protein. These mutants were expressed as an immature 100-kDa form processing oligosaccharides of the high mannose type. They were hardly expressed on the surface of cells, could not dimerize, lacked enzymatic activity and showed drastically reduced $t_{1/2}$.

These findings fit well with the preliminary β-propeller structure of the cysteine-rich domain of human DPPIV predicted by Abbott et al. [26]. According to this model, cysteines C326/C337, C383/C395, C445/C448 and C455/C473 are located pair-wise on different propeller blades. Propeller structures may be stabilized by intrablade disulfide bonds. As DPPIV belongs to a special subfamily of serine proteases, the prolyl oligopeptidases, it is predicted that the α/β-hydrolase fold is present and contains the catalytic domain [23,35,36]. This model does not have a disulfide bond within the carboxy-terminal domain, which is in accordance with the wild-type-like characteristics of mutants C650G and C763S.

In conclusion, our results suggest that cotranslational N-glycosylation and the formation of correct disulfide bonds is important for the attainment of a correctly folded, stable conformation of DPPIV.

Acknowledgements

This work was supported by a grant from the Deutsche Forschungsgemeinschaft Bonn (Sonderforschungsbereich 366), the Sonnenfeld-Stiftung and the Fonds der Chemischen Industrie, Frankfurt/Main.

References

1. Hopsu-Havu VK, Glenner GG. A new dipeptide naphthylamidase hydrolyzing glycyl-prolyl-beta- naphthylamide. Histochemistry 1966;7:197–201.
2. Hopsu-Havu VK, Makinen KK. The hydrolysis of aminoacid naphthylamides by the human seminal aminopeptidase. Arch Klin Exp Dermatol 1967;228:316–326.
3. Morimoto C, Schlossman SF. The structure and function of CD26 in the T-cell immune response. Immunol Rev 1998;161:55–70.
4. von Bonin A, Steeg C, Mittrucker HW, Fleischer B. The T-cell receptor associated zeta-chain is required but not sufficient for CD26 (dipeptidylpeptidase IV) mediated signaling. Immunol Lett 1997;55:179–182.
5. Buhling F, Kunz D, Reinhold D, Ulmer AJ, Ernst M, Flad HD, Ansorge S. Expression and functional role of dipeptidyl peptidase IV (CD26) on human natural killer cells. Nat Immun 1994;13:270–279.
6. Marguet D, Bernard AM, Vivier I, Darmoul D, Naquet P, Pierres M. cDNA cloning for mouse thymocyte-activating molecule. A multifunctional ecto-dipeptidyl peptidase IV (CD26) included in a subgroup of serine proteases. J Biol Chem 1992;267:2200–2208.
7. Misumi Y, Hayashi Y, Arakawa F, Ikehara Y. Molecular cloning and sequence analysis of human dipeptidyl peptidase IV, a serine proteinase on the cell surface. Biochim Biophys Acta 1992; 1131:333–336.
8. Kyouden T, Himeno M, Ishikawa T, Ohsumi Y, Kato K. Purification and characterization of dipeptidyl peptidase IV in rat liver lysosomal membranes. J Biochem Tokyo 1992;111:770–777.
9. Hutchinson DR, Halliwell RP, Lockhart JD, Parke DV. Glycylprolyl-p-nitroanilidase in hepato-

biliary disease. Clin Chim Acta 1981;109:83–89.
10. Vlasak R, Vilas U, Strobl B, Kreil G. cDNA cloning and expression of secreted Xenopus laevis dipeptidyl. Eur J Biochem 1997;247:107–113.
11. Elovson J. Biogenesis of plasma membrane glycoproteins. Tracer kinetic study of two rat liver plasma membrane glycoproteins in vivo. J Biol Chem 1980;255:5816–5825.
12. Danielsen EM. Dimeric assembly of enterocyte brush border enzymes. Biochemistry 1994;33: 1599–1605.
13. Jascur T, Matter K, Hauri HP. Oligomerization and intracellular protein transport: dimerization of intestinal dipeptidylpeptidase IV occurs in the Golgi apparatus. Biochemistry 1991;30: 1908–1915.
14. Ogata S, Misumi Y, Ikehara Y. Primary structure of rat liver dipeptidyl peptidase IV deduced from its cDNA and identification of the NH_2-terminal signal sequence as the membrane-anchoring domain. J Biol Chem 1989;264:3596–3601.
15. Ogata S, Misumi Y, Tsuji E, Takami N, Oda K, Ikehara Y. Identification of the active site residues in dipeptidyl peptidase IV by affinity labeling and site-directed mutagenesis. Biochemistry 1992;31:2582–2587.
16. David F, Bernard AM, Pierres M, Marguet D. Identification of serine 624, aspartic acid 702, and histidine 734 as the catalytic triad residues of mouse dipeptidylpeptidase IV (CD26). J Biol Chem 1993;268:17247–17252.
17. Bermpohl F, Loster K, Reutter W, Baum O. Rat dipeptidyl peptidase IV (DPP IV) exhibits endopeptidase activity with specificity for denatured fibrillar collagens. FEBS Lett 1998;428: 152–156.
18. Augustyns K, Bal G, Thonus G, Belyaev A, Zhang XM, Bollaert W, Lambeir AM, Durinx C, Goossens F, Haemers A. The unique properties of dipeptidyl-peptidase IV (DPP IV / CD26) and the therapeutic potential of DPP IV inhibitors. Curr Med Chem 1999;6:311–327.
19. Reutteer W, Baum O, Löster K, Fan H, Bork JP, Bernt K, Hanski Ch, Tauber R. Functional aspects of the three extracellular domains of dipeptidyl peptidase IV: Characterization of glycosylation events, of the collagen-binding site and of endopeptidase activity. In: Fleischer B. (eds) Dipeptidyl Peptidase IV (CD26) in Metabolism and the Immune Response. New York: Springer, 1995;55–78.
20. Hanski C, Huhle T, Gossrau R, Reutter W. Direct evidence for the binding of rat liver DPP IV to collagen in vitro. Exp Cell Res 1988;178:64–72.
21. Wesley UV, Albino AP, Tiwari S, Houghton AN. A role for dipeptidyl peptidase IV in suppressing the malignant phenotype of melanocytic cells. J Exp Med 1999;190:311–322.
22. von Bonin A, Huhn J, Fleischer B. Dipeptidyl-peptidase IV/CD26 on T cells: analysis of an alternative T-cell activation pathway. Immunol Rev 1998;161:43–53.
23. Dong RP, Tachibana K, Hegen M, Munakata D, Schlossman SF, Morimoto C. Determination of adenosine deaminase binding domain on CD26 and its immunoregulatory effect on T cell activation. J Immunol 1997;159:6070–6076.
24. Lambeir AM, Diaz Pereira JF, Chacon P, Vermeulen G, Heremans K, Devreese B, Van Beeumen J, De Meester I, Scharpe S. A prediction of DPP IV/CD26 domain structure from a physicochemical investigation of dipeptidyl peptidase IV (CD26) from human seminal plasma. Biochim Biophys Acta 1997;1340:215–226.
25. Goossens F, De Meester I, Vanhoof G, Hendriks D, Vriend G, Scharpe S. The purification, characterization and analysis of primary and secondary-structure of prolyl oligopeptidase from human lymphocytes. Evidence that the enzyme belongs to the alpha/beta hydrolase fold family. Eur J Biochem 1995;233:432–441.
26. Abbott CA, McCaughan GW, Gorrell MD. Two highly conserved glutamic acid residues in the predicted beta propeller domain of dipeptidyl peptidase IV are required for its enzyme activity. FEBS Lett 1999;458:278–284.
27. Löster K, Zeilinger K, Schuppan D, Reutter W. The cysteine-rich region of dipeptidyl peptidase IV (CD26) is the collagen-binding site. Biochem Biophys Res Commun 1995;217:341–348.

28. Pecci L, Cannella C, Pensa B, Costa M, Cavallini D. Cyanylation of rhodanese by 2-nitro-5-thiocyanobenzoic acid. Biochim Biophys Acta 1980;623:348–353.
29. Fan H, Meng W, Kilian C, Grams S, Reutter W. Domain-specific N-glycosylation of the membrane glycoprotein dipeptidylpeptidase IV (CD26) influences its subcellular trafficking, biological stability, enzyme activity and protein folding. Eur J Biochem 1997;246:243–251.
30. Dobers J, Grams S, Reutter W, Fan H. Roles of Cysteines in Rat Dipeptidyl Peptidase IV/CD26 in Processing and Proteolytic Activity. Eur J Biochem 2000;267:5093–5100.
31. Nagatsu T, Hino M, Fuyamada H, Hayakawa T, Sakakibara S. New chromogenic substrates for X-prolyl dipeptidyl-aminopeptidase. Anal Biochem 1976;74:466–476.
32. Loch N, Tauber R, Becker A, Hartel-Schenk S, Reutter W. Biosynthesis and metabolism of dipeptidylpeptidase IV in primary cultured rat hepatocytes and Morris hepatoma 7777 cells, Eur J Biochem 1992;210:161–168.
33. Chen W, Helenius J, Braakman I, Helenius A. Cotranslational folding and calnexin binding during glycoprotein synthesis. Proc Natl Acad Sci USA 1995;92:6229–6233.
34. Molianri M, Helenius A. Glycoproteins form mixed disulphides with oxidoreductases during folding in living cells. Nature 1999;402:90–93.
35. Abbott CA, Baker E, Sutherland GR, McCaughan GW. Genomic organization, exact localization, and tissue expression of the human CD26 (dipeptidyl peptidase IV) gene. Immunogenetics 1994;40:331–338.
36. Fulop V, Bocskei Z, Polgar L. Prolyl oligopeptidase: an unusual beta-propeller domain regulates proteolysis. Cell 1998;94:161–170.